Journal of Computational Neuroscience 19, 87–98, 2005

Dynamical Heterogeneity of Suprachiasmatic Nucleus Neurons Based on Regularity and Determinism

JAESEUNG JEONG
Department of Biosystems, Korea Advanced Institute of Science and Technology, Daejeon, South Korea 305-701

YONGHO KWAK
National Creative Research Initiative Center for Neurodynamics and Department of Physics, Korea University, Seoul, South Korea 136-701

YANG IN KIM
Department of Physiology and Neuroscience Research Institute, Korea University College of Medicine, Seoul, South Korea 136-701

KYOUNG J. LEE*
National Creative Research Initiative Center for Neurodynamics and Department of Physics, Korea University, Seoul, South Korea 136-701
kyoung@nld.korea.ac.kr

Received December 18, 2003; Revised February 24, 2005; Accepted March 4, 2005

Action Editor: Barry J. Richmond

Abstract. The suprachiasmatic nucleus (SCN) is known to be the master biological clock in mammals. Despite the periodic mean firing rate, interspike interval (ISI) patterns of SCN neurons are quite complex and irregular. The aim of the present study was to investigate the existence of nonlinear determinism in the complex ISI patterns of SCN neurons. ISI sequences were recorded from 173 neurons in rat hypothalamic slice preparations using a cell-attached patch recording technique. Their correlation dimensions (D_2) were estimated, and were then compared with those of the randomly-shuffled surrogate data. We found that only 16 neurons (16/173) exhibited deterministic ISI patterns of spikes. In addition, clustering analysis revealed that SCN neurons could be divided into two subgroups of neurons each having distinct values of coefficient of variation (CV) and skewness (SK). Interestingly, most deterministic SCN neurons (14/16) belonged to the group of irregularly spiking neurons having large CV and SK values. To see if the neuronal coupling mediated by the γ-aminobutyric acid (GABA), the major neurotransmitter in the SCN, contributed to the deterministic nature, we examined the effect of the $GABA_A$ receptor antagonist bicuculline on D_2 values of 56 SCN neurons. 8 SCN neurons which were originally stochastic became to exhibit deterministic characteristics after the bicuculline application. This result suggests that the deterministic nature of the SCN neurons arises not from GABAergic synaptic interactions, but likely from properties inherent to neurons themselves.

Keywords: suprachiasmatic nucleus, nonlinear determinism, interspike intervals, heterogeneity

*To whom correspondence should be addressed.

1. Introduction

The suprachiasmatic nucleus (SCN) contains pacemaker neurons imposing circadian rhythmicity in mammals (Meijer and Rietveld, 1989; Morin, 1994). The circadian rhythm of SCN neurons is expressed by the sinusoidal modulation of their mean firing rates. Individual SCN neurons are autonomous pacemaker cells that harbor an interconnected set of transcription-translation negative and positive feedback loops, which produce coordinated, rhythmic changes in expression of clock genes (for reviews, Reppert and Weaver, 2001, 2002). Spiking activity of SCN neurons follows this molecular clockwork, with higher mean firing rates during the day and lower firing rates at night (Inouye and Kawamura, 1979; Jagota et al., 2000; Schaap et al., 2003). Such circadian oscillation in action potential firing frequency is known to be crucial for the transmission of time information to other brain areas to impose circadian rhythmicity on physiological and behavioral activities (Schwartz et al., 1987; Newman et al., 1992; Shirakawa et al., 2001).

However, on a short time scale, the spiking activity of individual SCN neurons in the neuronal network is neither periodic nor modulated. Extracellular single unit measurements revealed that SCN neurons have several types of firing characteristics: regular, irregular, or burst-like (Cahill and Menaker, 1989; Groos and Hendriks, 1979; Shibata et al., 1984; Pennartz et al., 1998). The spontaneous firing rate of an SCN neuron incessantly varies ranging from 1.5 to 15 Hz, often accompanied by intermittent bursts (Gillette, 1991; Pennartz et al., 1998; Jagota et al., 2000; Schaap et al., 2003). Interspike intervals (ISIs) of SCN neurons are quite irregular and complex. How this complex spontaneous spiking activity of individual SCN neurons eventually leads to the long-range circadian rhythm is poorly understood.

As a first step toward understanding this issue, we investigated the firing patterns of individual SCN neurons and their underlying dynamics. In this study, we used nonlinear time series methods to determine whether the complex ISI patterns of SCN neurons are random or deterministic, a critical issue for understanding their cellular mechanisms underlying circadian rhythms. Whether temporal patterns of spikes are deterministic or not decides our approach to investigate the patterns and their underlying dynamics. Recently, nonlinear dynamical theory has shown that the irregularity of a time series may not necessarily result from a stochastic process. Systems of deterministic chaos can exhibit a very irregular behavior as stochastic systems do. Indeed, a number of recent studies have shown that irregular spiking activities recorded from various brain regions emerge from deterministic chaos (for reviews, McKenna et al., 1994; Rabinovich and Abarbanel, 1998; Faure and Korn, 2001; Segundo, 2003).

Nonlinear time series analysis has provided new tools detecting the presence of nonlinear determinism in a time series, which cannot be assessed by conventional spectral analysis. These are proven applicable to the study of ISI sequences obtained from neurons and neuronal ensembles (Sauer, 1994; Hegger and Kantz, 1997). In the present study, the correlation dimension (D_2) was used to detect the presence of nonlinear determinism in ISI sequences of SCN neurons in hypothalamic slices. Our analysis revealed that about 10% of the SCN neuronal population exhibits truly deterministic patterns of spikes, while the remaining population shows stochastic patterns.

There has been the hypothesis that the deterministic nature of neuronal spike trains, in general, arises from neuronal interactions. Rapp et al. (1985) and Sauer (1994) have proposed that the deterministic structure of ISI sequences with a few degrees of freedom can result from neural interactions in the presence of self-organizing and synchronizing influences. Neuronal interactions in a simple model network can, indeed, generate various types of oscillatory modes including a deterministic chaotic behavior in its ISI patterns (Chapeau-Blondeau and Chauvet, 1992; Lewis and Glass, 1992). Experimental evidences supporting this hypothesis have been also found in the rat spinal cord (Chang et al., 1994; Debus and Sandkuhler, 1996) and nigral dopamine neurons (Hoffman et al., 1995, 2001; Di Mascio et al., 1999b; Jeong et al., 2000, submitted). These studies demonstrated significant reductions in nonlinear determinism of ISI sequences after the interruption of neuronal couplings.

Although multiple ways of intercellular communications have been found in the SCN, the most significant neurochemical mediator for neuronal coupling is the γ-aminobutyric acid (GABA) (Okamura et al., 1989; Moore and Speh, 1993). Thus, in order to determine whether $GABA_A$ receptor-mediated synaptic couplings contribute to the deterministic nature, we applied the $GABA_A$ receptor antagonist bicuculline to SCN neurons and evaluated subsequent changes in the deterministic nature of ISI sequences. Eight

stochastic SCN neurons became to exhibit deterministic characteristics, and other stochastic neurons showed a marked decrease in the complexity of spiking patterns. These results suggest that the deterministic behavior of SCN neurons pertain to the individual SCN neurons themselves.

2. Materials and Methods

2.1. Animals and Brain Slice Preparation

Male Sprague-Dawley rats ($n = 52$; 40–100 g) were housed in a temperature-controlled room (25–27°C) under a 12/12-hr light/dark cycle (light on 07:00–19:00) for at least 2 weeks prior to use. The rats were anesthetized with Nembutal (6 mg/100 g body weight) in the daytime of subjects, and then the brains were quickly removed and submerged in ice-cold artificial cerebrospinal fluid [ACSF (mM): 124NaCl, 26$NaHCO_3$, 3KCl, 2.4$CaCl_2$, 1.3$MgSO_4$, 1.25NaH2PO_4, 10Glucose, 95% O_2, and 5% CO_2 saturation]. Using a vibrating tissue slicer (Vibratome 1000, Technical Products International, USA), a block of hypothalamic tissue was cut into slices coronally at the thickness of 120–150 μm. The slices containing the SCN were transferred to a recording chamber perfused by the same ACSF at the flow rate of 1.0–1.5 ml/min. The experimental procedures described above were in accordance with the guideline set by the Korea University College of Medicine Animal Research Policies Committee.

2.2. Extracellular Recording

After 1-hr incubation in the recording chamber, extracellular recordings were commenced at room temperature (25–27°C). The recording electrodes made of borosilicate tubings (Sutter Inst. Co. USA) had a tip diameter of 2–4 μm with a resistance of 3–5 Mohm. Cell-attached patch (CAP) configuration without membrane rupture was achieved for extracellular, single-unit recording. In a CAP mode, a single action potential caused a transient capacitive current over the patch of membrane sucked into the pipette tip. This was recorded under voltage clamp conditions with a pipette potential of 0 mV. The recordings were performed using Axo-patch 200B amplifier (Axon Instruments, USA) in track mode from 173 SCN neurons for 20–40 minutes, and the ISI data were stored using pClamp software. The mean number of data points was $7{,}356 \pm 2{,}961$ (range: 1,422–19,213). For each recording, first two minute of data were discarded to ensure the stationarity of the ISI sequences as possible. Before the analysis, we have divided each ISI sequence into 1 min segments and estimated the means and variances of segments to ensure the stationarity of the ISI sequence.

2.3. Nonlinear Dynamical Analysis

The correlation dimension (D_2) reflects the number of independent variables that are essential for describing the dynamics of the concerned system. D_2 values of ISI sequences were estimated using the Grassberger-Procaccia algorithm (see Appendix). The D_2 of a deterministic system is preserved as the embedding dimension increases, whereas that of a stochastic system increases without any saturation.

The surrogate data test was used to confirm the presence of the deterministic nature in the ISI sequences of SCN neurons. Surrogate data are a randomized sequence of the original data with all nonlinear determinism that may be present destroyed but their amplitude histogram and power spectrum preserved (Theiler, 1992; Schreiber and Schmitz, 2000). Thus, a statistically significant difference in the D_2 values between original data and the surrogate data would indicate the presence of nonlinear determinism in the original data. In our analysis, the D_2 estimation was applied to each raw ISI data set and 19 different sets of surrogates. Pairwise t-tests of the difference between the D_2 values of the original ISI sequences and the mean D_2 values of their 19 surrogates were applied to test the null hypothesis of a stochastic behavior.

In addition, the significance S was also introduced to quantify the significance of the deterministic behavior (Longtin, 1993; Shen et al., 2003; Theiler et al., 1992; Rapp et al., 1993; Hoffman et al., 1995). The S was defined by

$$S + \frac{|\langle D_{2s}\rangle - D_2|}{\sigma_s}, \tag{1}$$

where $\langle D_{2S}\rangle$ denotes the mean D_2 value of the 19 surrogate data, D_2 was the correlation dimension of the original data set, and σ_s was the standard deviation of D_2 values of the surrogates. If nonlinear determinism is present, D_2 should be significantly less than $\langle D_{2s}\rangle$. An S-value larger than 1.96 at an optimal embedding dimension estimated using the false nearest neighbor method proposed by Kennel et al. (1992), indicates the

presence of deterministic behavior in the original data (with a 0.95 level of significance), as suggested by Shen et al. (2003). All numerics were expressed by mean ± S.D. All tests of statistical significance were two-tailed. The algorithm is briefly presented in the Appendix. All tests of statistical significance were two-tailed.

3. Results

3.1. Nonlinear Determinism in ISI Sequences of SCN Neurons

A typical ISI sequence generated by an SCN neuron is shown in Fig. 1. All observed neurons ($n = 173$) produced highly irregular ISI sequences, whose distributions were unimodal with a mean of 0.24 ± 0.09 sec. While the majority of the neurons studied here had a normally-distributed ISI histogram, about 30% of the population exhibited a skewed ISI histogram towards longer ISI values.

D_2 values were estimated for all data sets as the embedding dimension (d_e) increased from 2 to 15. Among 173 neurons, 16 neurons exhibited saturated D_2 values as the d_e increased. Figure 2A presents the local slopes of correlation integrals (the local D_2 profile) for the ISI sequence obtained from a deterministic SCN neuron as a function of log-scaled r for $d_e = 5$, 10, and 15. The approximate value of the plateau (scaling region) in the local D_2 profile is the D_2 value for the data at a particular embedding dimension. The D_2 value of this neuron, estimated by linear regression analysis, was 5.38. This indicates that spiking activity of this neuron was quite deterministic with finite degrees of freedom, despite the high irregularity of the ISI sequence. In contrast, the D_2 values of its surrogate data increased without saturation as the d_e increased (Fig. 2B). The D_2 differences between the original data and their surrogate data increased as the de increased, as shown in Fig. 2C. 16

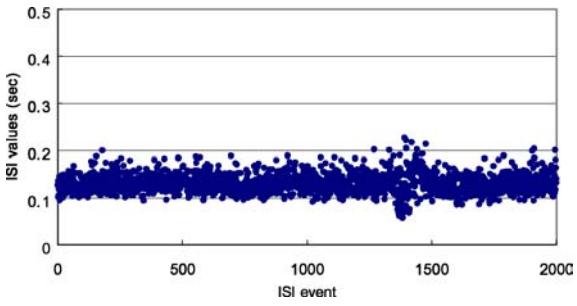

Figure 1. The ISI sequence of an SCN neuron as a function of time.

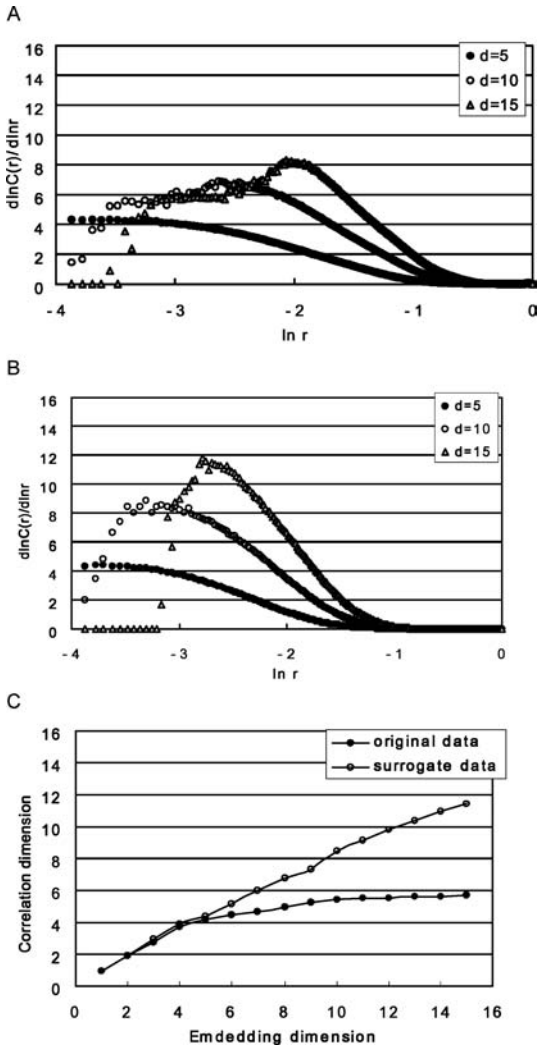

Figure 2. The D_2 profiles of (A) the ISI sequence recorded from a typical deterministic SCN neuron and (B) the corresponding surrogate data as the embedding dimension increases. (C) The average D_2 values of the original ISI data and their surrogate data as a function of the embedding dimension.

neurons had long plateau enough to ensure nonlinear determinism. The mean D_2 values of the 16 deterministic neurons were 8.15 ± 1.36. The S-scores of the D_2 values for 16 ISI data sets were estimated at optimal embedding dimensions. Using the false nearest neighborhood method, the optimal embedding dimensions for these sixteen ISI data sets were estimated as 10–12. The mean S-score was 8.87 ± 1.59, indicating that the 16 SCN neurons generated deterministic ISI patterns, although it is relatively high-dimensional (dimension range: 5.5–10.2). Paired t-test also supported the results from the S-score analysis ($0.0001 < P$).

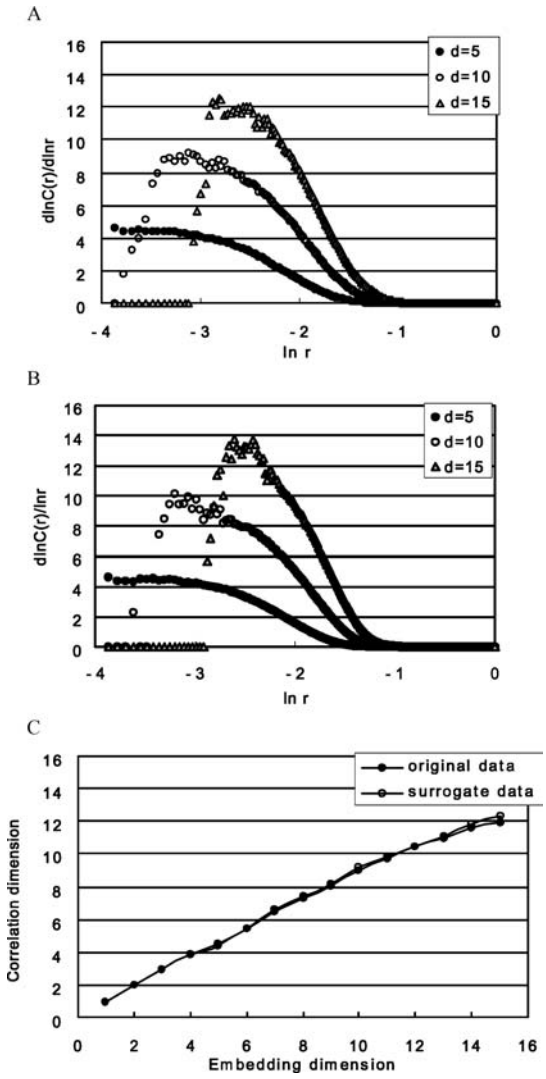

Figure 3. The D_2 profiles of (A) the ISI sequence recorded from a stochastic SCN neuron and (B) their surrogate data as the embedding dimension increases. (C) The average D_2 values of the original ISI data and their surrogate data as a function of the embedding dimension.

The other neurons (157/173) exhibited stochastic ISI patterns. Figure 3A presents the local D_2 profiles for the ISI data of a typical stochastic neuron at $d_e = 5$, 10, and 15. Their D_2 values increased without any saturation as the de increased. The D_2 profiles of the corresponding surrogate data were very similar to those of the original data (Fig. 3B). D_2 values for the original ISI data and their surrogate data showed no significant differences as the de increased (Fig. 3C). The mean S-scores of the D_2 for these ISI data sets were 0.25 ± 0.12 at the embedding dimension 12, indicating that ISI sequences obtained from these 157 SCN neurons are not deterministic.

3.2. *Electrophysiological Heterogeneity of SCN Neurons*

The regularity in spontaneous firing patterns of neurons is usually quantified by the coefficient of variation (CV) in spike intervals, which is defined as the standard deviation divided by the mean ISI. From a statistical point of view, higher CV values of ISI sequences indicate more irregular firing patterns. CV values of 173 SCN neurons were found to distribute over a significantly wide range: 113 neurons had relatively low CV values ranging from 0.1–0.4, indicating regularly spiking neurons. The other group of 60 neurons showed high CV values (range: 0.4–0.8), indicative of irregularly spiking neurons. This result raised the possibility that a subgroup of relatively irregular neurons is present in the SCN.

Based on the histogram and regularity analyses of ISIs, we investigated the possibility of the presence of subgroups in the populations of SCN neurons. Figure 4 clearly demonstrates that SCN neurons are divided into two clusters in the parametric space of CV and skewness (SK): one group with skewed ISI histograms towards more long ISIs ($2.0 < \mathrm{SK} < 10.0$) and high CV values ($0.4 < \mathrm{CV} < 0.8$), which was denoted as 'cluster I', and the other group with normally-distributed ISI histograms ($-1.0 < \mathrm{SK} < 2.0$) and low CV values ($0.1 < \mathrm{CV} < 0.4$), which was labeled 'cluster II' (Fig. 4).

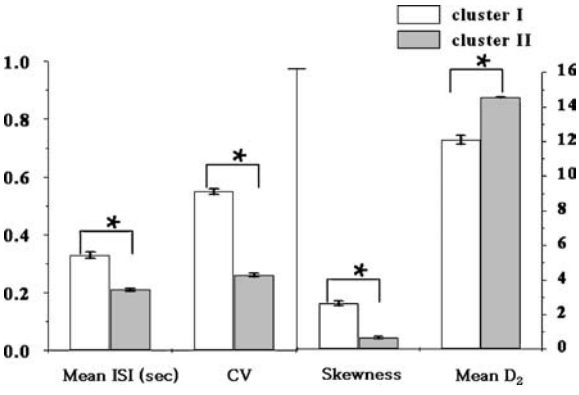

Figure 4. Comparison of firing properties (mean ± standard errors) of SCN neurons between cluster I ($n = 60$) and II ($n = 113$). The left y-axis indicates the amplitudes of mean ISI (sec) and CV values, and the right y-axis the amplitudes of SK and the mean D_2 values.

Table 1. Spike train properties (mean ± standard deviations) per cluster of SCN neurons ($n = 173$).

Parameters	Cluster I	Cluster II	t-value
Number of cells	60	113	–
Mean ISI (sec)	0.33 ± 0.14	0.21 ± 0.06	6.14*
Skewness	2.64 ± 1.76	0.67 ± 0.86	7.18*
CV	0.55 ± 0.12	0.26 ± 0.08	13.92*
Mean D_2	12.11 ± 3.54	14.56 ± 1.56	−4.59*
Probability of deterministic neurons	14/60	2/113	–

Student t-test; CV: coefficient of variation
*$P < 0.001$

Table 2. Detailed description of the changes in electrophysiological properties (mean ± standard deviations) of SCN neurons by the bicuculline application ($n = 56$).

Parameters	Normal condition	Bicuculline condition	t-test
Mean ISI (sec)	0.22 ± 0.06	0.17 ± 0.05	−0.85*
SK	1.53 ± 2.58	2.41 ± 6.43	-0.81^{NS}
CV	0.39 ± 0.25	0.48 ± 0.50	-0.86^{NS}
Mean D_2	14.15 ± 1.19	12.93 ± 2.69	2.28*

Paired t-test.
CV: Coefficient of variation; SK: skewness; NS: not significant; *$P < 0.05$.

In addition, we quantitatively examined the presence of two subgroups using hierarchical clustering analysis. The parameters, CV and SK, were standardized and subjected to the hierarchical tree clustering. Individual neurons were represented as terminal branch point along the bottom of dendrogram and labeled. When the linkage distance gradually increases, successive branch points represent clusters of increasing size and dissimilarity. The main binary branching was found at a proper linkage distance. The more detailed algorithm of the hierarchical clustering analysis is present in the Appendix.

The significant differences in CV and SK values between two clusters were confirmed, as shown in Table 1 ($P < 0.001$; Student t-test). In a *post hoc* analysis, cluster I was found to have a longer mean ISI and a smaller mean D_2 value than those of cluster II (Fig. 5). More surprisingly, the majority of deterministic SCN neurons (14/16) belonged to cluster I, while the other larger group (cluster II) of regularly spiking SCN neurons having small SK and CV values are mostly stochastic. These findings indicate that SCN neurons are heterogeneous in properties of firing patterns.

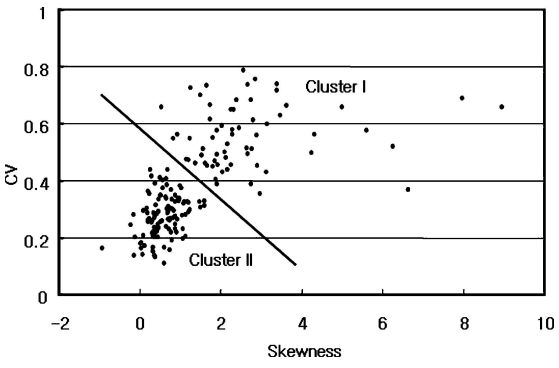

Figure 5. Plot of CV of interspike intervals versus SK for 173 SCN neurons. Two clusters can be discerned having small CV and SK values, and large CV and SK values, respectively. The values on the axes are not standardized.

3.3. *The Bicuculline Effect on Nonlinear Determinism in SCN Neurons*

Since the GABA is the major neurotransmitter of the SCN, bicuculline was applied to examine the role of $GABA_A$ receptor-mediated synaptic couplings in the nonlinear deterministic behavior of some SCN neurons. Bath application of bicuculline (30 μM for 20 min) was performed for 56 SCN neurons selected from 173 neurons after a baseline recording (15–20 min) in a normal condition.

The statistical measures and D_2 values of 56 ISI sequences were evaluated before and after the bicuculline application, and summarized in Table 2. The mean ISI was significantly decreased after the bicuculline application, whereas the CV and SK were not (Table 2). The reduction in the mean ISI indicates that spontaneous $GABA_A$ receptor-mediated inputs do inhibit the SCN neurons. In normal conditions, 54 neurons out of 56 SCN neurons exhibited stochastic activity and only 2 neurons showed deterministic activity. The most significant finding was that 8 stochastic SCN neurons (8/54) in normal conditions turned to have nonlinear determinism (mean D_2:7.92 ± 0.73 at $d_e = 12$) after the bicuculline application, while the remaining stochastic SCN neurons (46/54) showed a significant decrease in D_2 values (Fig. 6). Since the D_2 reflects the number of degrees of freedom, this result indicates that the spiking patterns of SCN neurons exhibit a reduction in the dimension of the spiking dynamics. It is noted that, for

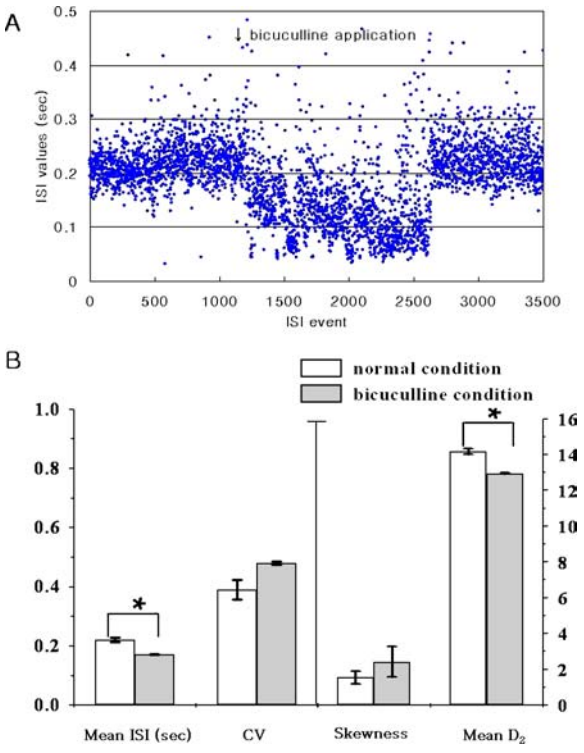

Figure 6. (A) The ISI sequence of an SCN neuron as a function of time in a normal condition, during the bicuculline application (30 μM for 20 min), and in a recovery condition. (B) Changes in firing properties (mean $\pm$ standard errors) of SCN neurons ($n = 56$) by the bicuculline application. The left y-axis indicates the amplitudes of mean ISI (sec) and CV values, and the right y-axis the amplitudes of SK and the mean D_2 values.

the 8 SCN neurons, their ISI histograms became to be more skewed towards to long ISIs, and their CV values were increased. Furthermore, two deterministic neurons (2/56) in normal conditions still had the deterministic structure after the bicuculline application. Taken together, these results suggest that the deterministic nature of SCN neurons does not arise from $GABA_A$ receptor-mediated synaptic couplings, but from intrinsic properties of the neurons.

4. Discussion

The mechanisms underlying variability and complexity in spiking patterns of neurons are an important issue in neurophysiology and computational neuroscience (Softky and Koch, 1993; Troyer and Miller, 1997; Shadlen and Newsome, 1998). A number of studies have demonstrated that ISI sequences are very variable, but not quite random (for reviews, Rapp et al., 1994; Faure and Korn, 2001; Segundo, 2003). A deterministic (or predictable) temporal structure of ISI sequences has been repeatedly reported in various neuronal preparations (Mpitsos et al., 1988; Hayashi and Ishizuka, 1992; Chang et al., 1994; Hoffman et al., 1995, 2001; Debus and Sandkuhler, 1996; De Menendez et al., 1997; Di Mascio et al., 1999a, 1999b; Wan et al., 2000; Jeong et al., 2000; Suzuki et al., 2000; Lovejoy et al., 2001). The present study demonstrates that some SCN neurons also generate deterministic ISI sequences. In other words, interspike intervals and overall patterns of neuronal spike trains in some SCN neurons are generated and/or exquisitely regulated by deterministic rules, regardless of their highly irregular and complex behavior.

What is the origin of nonlinear determinism found in ISI sequences of SCN neurons? Our finding that the deterministic behavior of SCN neurons is persistent during the synaptic blockade by bicuculline indicates that the deterministic nature does not arise from $GABA_A$ receptor-mediated synaptic couplings. Rather, the emergence of the determinism in stochastic SCN neurons during the bicuculline application suggests that nonlinear determinism arises from intrinsic properties of SCN neurons themselves. Here, synaptic inputs may act as a stochastic noise source in the spiking activity of SCN neurons, based on the finding of the overall decrease in D_2 values during the GABA synaptic blockade. This result is not in accordance with the hypothesis that the deterministic nature of neuronal spike trains emerges from neuronal interactions (Rapp et al., 1985; Chapeau-Blondeau and Chauvet, 1992; Lewis and Glass, 1992; Sauer, 1994). However, it is consistent with previous SCN studies reporting that individual SCN neurons are an independent, autonomous circadian oscillator by itself (Welsh et al., 1995; Liu et al., 1997). It is noted that Lovejoy et al. (2001) draw a similar conclusion on nigral dopamine neurons that the irregular pattern of firing arises not from extrinsic inputs or neuronal interactions, but rather from the intrinsic, deterministic dynamics of neurons.

The association between nonlinear determinism observed in ISI sequences of SCN neurons and circadian rhythms is not known. However, deterministic rules underlying ISI sequences are possibly significant for SCN neurons in imposing circadian rhythms on their spiking patterns on a longer time scale. We speculate that SCN neurons employ some deterministic rules to regulate

interspike intervals to impose circadian rhythmicity on their overall firing patterns.

However, at this point, we should note that the majority of SCN neurons exhibit stochastic behaviors in their ISI sequences, and that only about 10% of the SCN neurons show the deterministic characteristics. How can these stochastic SCN neurons impose circadian rhythmicity on their mean firing rates? A possible explanation is that stochastic SCN neurons are non-rhythmic cells, but can be driven to be rhythmic by clock cells, which are likely deterministic neurons, through synaptic interactions. It is well known that the SCN consists of rhythmic clock cells and non-rhythmic cells (Lee et al., 2003). Another possibility is that stochastic SCN neurons have long-term correlations among ISIs, which can produce modulations of mean firing rates. Although they produce spiking patterns through a stochastic process, correlations within ISIs over various time scales, so called $1/f$ power-law (fractal) activity, can modulate the mean firing rates to impose circadian rhythmicity.

Another interesting finding is that SCN neurons are heterogeneous in properties of regularity and nonlinear determinism. Two subgroups are identified: a small group (cluster I) of irregularly spiking SCN neurons having relatively large SK and CV values and the other larger group (cluster II) of regularly spiking SCN neurons having small SK and CV values. Most deterministic neurons belong to cluster I, i.e. the irregularly spiking neuron group. This result is quite consistent with the earlier findings of Pennartz et al. (1998). They have examined, using a current-clamp recording technique, electrophysiological and morphological properties of SCN neurons in hypothalamic slices to find that SCN neurons can be partitioned into three clusters, viz. cluster I being characterized by monophasic spike afterhyperpolarizations (AHPs) and irregular firing of high CV values, cluster II with biphasic spike AHPs and relatively regular firing with low CV values, and cluster III with large rebound depolarizations and biphasic spike AHPs. Based on the values of CV and mean ISIs, the cluster I and II defined in our study seem to correspond to the cluster I and II denoted by Pennartz group, respectively.

Anatomical and functional heterogeneity within the SCN have been empirically observed. It was initially reported that SCN-lesioned animals continue to be rhythmic so long as at least 20% of SCN neurons remain intact and damage to pathways rostral to the SCN is more critical for rhythmicity than damage to caudal pathways (Rusak, 1977; Harrington et al., 1993). The SCN is structurally heterogeneous and subdivided into two parts, the ventrolateral and dorsomedial areas (Moore, 1996; Moga and Moore, 1997). The ventrolateral area contains vasoactive intestinal polypeptide (VIP), substance P, and gastrin-releasing peptide, while the dorsomedial area contains arginine vasopressin (AVP) (Moore, 1996; van Esseveldt et al., 2000). More interestingly, Pennartz et al. (1998) using immunohistochemical staining for AVP found that AVP-positive neurons exhibit more prominent circadian rhythms in spontaneous firing rate than those of AVP-negative neurons and most AVP-positive neurons belong to cluster I. Furthermore, Schaap et al. (1999, 2003) demonstrated that irregularly firing neurons in cluster I have circadian rhythms, whereas cluster II neurons do not participate in the expression of circadian rhythmicity. These findings might be associated with our result that cluster I neurons are mainly deterministic, whereas cluster II neurons are stochastic. If this is the case, we can speculate that the deterministic SCN neurons in cluster I act as rhythmic clock cells while the most stochastic neurons in cluster II are non-clock cells and that the nonlinear determinism observed in cluster I neurons in the present study is associated with cellular mechanisms for the generation of circadian rhythms. Recently, it was found that AHP in cluster I neurons regulates the firing rate in a circadian manner and that apamin- and iberiotoxin-insensitive $K_{(Ca)}$ channels, which are involved in the AHP mechanism, are subject to diurnal modulation by the circadian clock (Cloues and Sather, 2003). This modulation might either directly or indirectly lead to the expression of a circadian rhythm in spiking frequency. Thus, there is a possibility that the nonlinear determinism in cluster I neurons is related to the AHP mechanism, which should be further investigated.

The heterogeneity of nonlinear determinism in SCN neurons suggests that the SCN is composed of distinct neuronal subgroups each of which makes a unique functional contribution to the circadian timing. Thus, the structural and functional heterogeneity of the SCN should be considered particularly for a computational modeling study of the SCN (Moore and Silver, 1998; Hamada et al., 2001). Recently, Antle et al. (2003) proposed an SCN model that incorporates nonrhythmic 'gate' cells and rhythmic oscillator cells with a wide range of periods. The gate cells provide daily input to oscillator cells and are in turn regulated directly or indirectly by the oscillator cells. In their model, individual

oscillators with initial random phases are able to self-assemble so as to maintain coordinated, rhythmic output.

Finally, we should mention as a limitation of the current study that the length of ISI sequences used in this study is relatively short for producing reliable results in correlation-dimension estimation, because spiking dynamics of SCN neurons might be high-dimensional. Nonlinear dynamical methods require large number of data points to reconstruct the whole dynamics underlying neural activity in a high-dimensional phase space from ISI sequences (Jeong et al., 2002). With short time series, the phase space is so sparsely populated that neighborhoods of trajectories in the embedding space are poorly defined (Kantz and Schreiber, 1995). Furthermore, the application of these methods can lead to spurious results, if the time series under study is non-stationary. However, acquiring this large number of data points from a stationary time series is almost impossible when working with physiological systems. There might be a tradeoff between the necessary number of data points for nonlinear dynamical methods and stationarity in the time series. In this study, we experienced that ISI neuronal sequences over 6,000 data points having about 6–8 degrees of freedom might produce consistent results in the determinism test, in particular using both correlation dimension and surrogate data methods, and that they might maintain the statistical stationarity based on mean and variance estimation.

Another limitation is that the temperature in the recording chamber is 25–27°C which is different from that in vivo. Since temperature may affect the spiking dynamics of the SCN neurons, analysis of the ISI sequences in SCN neurons recorded at high temperature similar to in-vivo situation is further required to ensure the results on spiking dynamics of the SCN neurons in this study.

In conclusion, a small but significant number of SCN neurons are found to be deterministic in their firing temporal patterns, whereas most SCN neurons show stochastic properties. In addition, most deterministic neurons belong to a group of irregularly firing neurons. For further investigation, the biochemical, electrophysiological, and morphological properties of SCN neurons—in particular for deterministic neurons—will be examined to improve our understanding of the functional role of distinct groups of SCN neurons and to develop a more reliable computer model for the SCN.

Appendix

Nonlinear Dynamical Analysis and D_2 Estimation

Nonlinear analyses are usually performed in the phase-space. In the n-dimensional phase space, each state of the system corresponds to a single point in the phase space whose n coordinates are the values assumed by the governing variables for this specific state. If the system is observed through time, the sequence of points in the phase space forms a dynamical trajectory. This trajectory fills a subspace of the phase space, which is called the system's attractor.

However, in most biological systems, we are unable to obtain the actual underlying equations that generate complex behaviors, but only to observe temporal sequences of events $\{x(t)\}$. Thus, the attractor is reconstructed in the phase space from the observed sequences $\{x(t)\}$ by plotting delay coordinates in what is referred to as an embedding procedure (Eckmann and Ruelle, 1985). The delay coordinates $y(t) = [x(t), x(t + T), \ldots, x(t + (d - 1)T)]$ are constructed from an observed single time series $x(t)$, where T is the time delay and d is the embedding dimension, to unfold the projection back to a multivariate phase space that is a representation of the original system. An attractor reconstructed in an embedding procedure by using delay coordinates from a single time series $x(t)$ is topologically equivalent to the original dynamical system (Takens, 1981). Recently a number of studies have shown that nonlinear dynamical analysis is applicable to ISI sequences recorded from neurons or neuronal populations (Longtin, 1993; Chang et al., 1994; Rapp et al., 1994; Sauer, 1994; Schiff et al., 1994; Hegger and Kantz, 1997).

For the time delay T, the first local minimum of the average mutual information between the set of measurement $x(t)$ and $x(t + T)$ are often used. Mutual information measures linear and nonlinear dependence of two variables (Fraser and Swinney, 1986). However, for most ISI data sets, the average mutual information at one event interval is the first local minimum. Thus, T is set at one for ISI data sets.

Using the Grassberger-Procaccia algorithm (GPA), we evaluated the D_2 of the attractors from the delay coordinates obtained by ISI sequences of SCN neurons (Grassberger and Procaccia, 1983). In this algorithm, the D_2 calculation is based on determining the relative number of pairs of points in the phase-space data set that are separated by a distance less than r. It is

computed from

$$D_2 = \lim_{r\to 0} \lim_{N\to\infty} \frac{\log C(r, N)}{\log r}, \quad (2)$$

where the correlation integral $C(N, r)$ is defined by

$$C(r, N) = \frac{2}{(N - W)(N - 1 - W)} \times \sum_{i=1}^{N} \sum_{j=i+1+W}^{N} \theta(r - |\vec{x}_i - \vec{x}_j|), \quad (3)$$

where x_i and x_j are the points of the trajectory in the phase space, N is the number of data points in the phase space, the distance r is a radius around each reference point x_i, and θ is the Heaviside function, defined as 0 if $x < 0$, and 1 if $x \geq 0$. W denotes the Theiler correction (Theiler, 1986), which was used to correct for temporal correlations. A short plateau can be detected in the D_2 curve of ISI sequences for an appropriate combination of small values of delay time and Theiler correction W.

For small r, a scaling property is exhibited: $C(N, r) \propto r^{D_2}$. For a self-similar (fractal) attractor the local scaling exponent is constant, and this is called a scaling region. If this plateau is present over a significant long range, the scaling exponent can be used as an estimate of the D_2. C(N, r) is plotted against r on a log-log scale, and the D_2 is given by the slope of this curve over a selected range of r. In this study, the slope of the correlation integral curve in the scaling region was estimated by a linear regression method. We used a modification, proposed by Kantz and Schreiber (1997), of the GPA to removes pairs of points that are temporally close from consideration.

False Nearest Neighbor Method

The false nearest neighbor method utilizes geometric principles to determine the minimum embedding dimension. Takens (1981) have demonstrated that an embedding dimension of $2D + 1$ is generally sufficient to guarantee the proper reconstruction of the phase space dynamics, where D is the dimension of the attractor. Proper reconstruction means that the phase space trajectories are unfolded, and that orbits do not cross. In other words, the projection of system trajectories that is too low in dimension results in neighbor points that would not be neighbors in the case of proper reconstruction. The algorithm for estimating the minimum embedding dimension is based on the idea that, in the passage from dimension d to dimension $d + 1$, one can differentiate between points on the orbit that are true neighbors and those that are false (Kennel et al., 1992). A false neighbor is a point in the data set that is a neighbor only because we are viewing the orbit (the attractor) in too small an embedding space ($d < d_{\min}$). When we have achieved a large enough embedding space ($d \geq d_{\min}$), all neighbors of every point in the orbit of the multi-variate phase space will be true neighbors. The detailed algorithm is in the paper of Kennel et al. (1992) or Jeong et al. (1998).

Clustering Analysis

Grouping of neurons was performed by using hierarchical cluster analysis (SPSS version 10.0). Although this method does not allow rigorous conclusions about groupings of neurons, it provides an objective classification tool for SCN neurons based on their electrophysiological properties. Hierarchical clustering operates on a matrix that contains a measure for the dissimilarity between values of parameters for all pairs of neurons within the overall population. Dissimilarities are expressed as Euclidean distances in a space whose dimensions are the same as the number of parameters taken into account. These distances are computed on the basis of standardized values to remove the effect of scaling differences between parameters according to the following transformation: standardized value = (raw value − mean)/standard deviation. The clustering algorithm groups individual neurons into hierarchically nested clusters with increasing linkage distance. The linkage distance provides a criterion for progressively joining together neurons with increasing dissimilarity. When linkage distance is short, similar neurons are joined into a low-level cluster. High linkage distances yield large clusters of more dissimilar neurons, often spanning multiple lower branches of the dendrogram. In our analysis, the CV and SK were used as possible criteria to distinguish groups of neurons. The linkage rule used for joining small into larger clusters was weighted pair-group averaging (i.e. the criterion for cluster linking was derived from the average distance between all pairs of objects in two different clusters, using the size of each cluster as a weight factor) because of the large differences in size of the clusters.

Acknowledgment

This work was supported by Creative Research Initiatives of the Korean Ministry of Science and Technology.

References

Antle MC, Foley DK, Foley NC, Silver R (2003) Gates and oscillators: A network model of the brain clock. Journal of Biological Rhythms 18: 339–350.

Cahill GM, Menaker M (1989) Responses of the suprachiasmatic nucleus to retinohypothalamic tract volleys in a slice preparation of the mouse hypothalamus. Brain Research 479: 65–75.

Chang T, Schiff SJ, Sauer T, Gossard JP, Burke RE (1994) Stochastic versus deterministic variability in simple neuronal circuits: I. Monosynaptic spinal cord reflexes. Biophysical Journal 67: 671–683.

Chapeau-Blondeau F, Chauvet G (1992) Stable oscillatory and chaotic regimes in the dynamics of small neural networks with delay. Neural Networks 5: 735–743.

Cloues RK, Sather WA (2003) Afterhyperpolarization regulates firing rate in neurons of the suprachiasmatic nucleus. Journal of Neuroscience 23: 1593–1604.

De Menendez LA, Prida L, Stollenwerk N, Sanchez-Andres JV (1997) Bursting as a source for predictability in biological neural network activity. Physica D 110: 323–331.

Debus S, Sandkuhler J (1996) Low dimensional attractors in discharges of sensory neurons of the rat spinal dorsal horn are maintained by supraspinal descending systems. Neuroscience 70: 191–200.

Di Mascio M, Di Giovanni G, Di Matteo V, Esposito E (1999a) Reduced chaos of interspike interval of midbrain dopaminergic neurons in aged rats. Neuroscience 89: 1003–1008.

Di Mascio M, Di Giovanni G, Di Matteo V, Esposito E (1999b) Decreased chaos of midbrain dopaminergic neurons after serotonin denervation. Neuroscience 92: 237–243.

Eckmann JP, Ruelle D (1992) Fundamental limitations for estimating dimensions and Lyapunov exponents in dynamical systems. Physica D 56: 185–187.

Faure P, Korn H (2001) Is there chaos in the brain? Concepts of nonlinear dynamics and methods of investigation. Comptes Rendus de l'Academie des Sciences III 324: 773–793.

Fraser AM, Swinney HL (1986) Independent coordinates for strange attractors from mutual information. Physical Review A 33: 1134–1140.

Gillette MU (1991) SCN electrophysiology in vitro: Rhythmic activity and endogenous clock properties. In: DC Klein, RY Moore, SM Reppert, eds. Suprachiasmatic Nucleus: The Mind's Clock. Oxford University Press, New York, NY, pp. 125–143.

Grassberger P, Procaccia I (1983) Measuring the strangeness of strange attractors. Physica D 9: 189–208.

Groos GA, Hendriks J (1979) Regularly firing neurones in the rat suprachiasmatic nucleus. Experientia 35: 1597–1598.

Hamada T, LeSauter J, Venuti JM, Silver R (2001) Expression of Period genes: Rhythmic and nonrhythmic compartments of the suprachiasmatic nucleus pacemaker. Journal of Neuroscience 21: 7742–7750.

Harrington ME, Rahmani T, Lee CA (1993) Effects of damage to SCN neurons and efferent pathways on circadian activity rhythms of hamsters. Brain Research Bulletin 30: 655–669.

Hayashi H, Ishizuka S (1992) Chaotic nature of bursting discharges in the Onchidium: Pacemaker neurons. Journal of Theoretical Biology 156: 269–291.

Hegger R, Kantz H (1997) Embedding of sequences of time intervals. Europhysics Letters 38: 267–272.

Hoffman RE, Shi WX, Bunney BS (1995) Nonlinear sequence-dependent structure of nignal dopamine neuron interspike interval firing patterns. Biophysical Journal 69: 128–137.

Hoffman RE, Shi WX, Bunney BS (2001) Anatomic basis of sequence-dependent predictability exhibited by nigral dopamine neuron firing patterns. Synapse 39: 133–138.

Inouye ST, Kawamura H (1979) Persistence of circadian rhythmicity in a mammalian hypothalamic "island" containing the suprachiasmatic nucleus. Proceedings of National Academy of Sciences USA 76: 5962–5966.

Jagota A, de la Iglesia HO, Schwartz WJ (2000) Morning and evening circadian oscillations in the suprachiasmatic nucleus in vitro. Nature Neuroscience 3: 372–376.

Jeong J, Kim SY, Han SH (1998) Nonlinear analysis of chaotic dynamics underlying EEGs in patients with Alzheimer's disease. Electroencephalography and Clinical Neurophysiology 106: 220–228.

Jeong J, Peterson BS, Gore JC, Hoffman RE, Shi WX, Bunny BS (2000) Bursting as a source of nonlinear deterministic structure in interspike interval firing patterns of nigral dopamine neurons. Society for Neuroscience Abstract 26.

Jeong J, Gore JC, Peterson BS (2002) A method for determinism in short time series, and its application to stationary EEG. IEEE Trans Biomed Eng 49(11): 1374–1379.

Jeong J, Shi WX, Hoffman RE, Gore JC, Bunny BS, Peterson BS. The origin of nonlinear determinism in interspike interval firing patterns of nigral dopamine neurons (submitted).

Kantz H, Schreiber T (1995) Dimension estimates and physiological data. Chaos 5(1): 143–154.

Kantz H, Schreiber T (1997) Nonlinear time series analysis. Cambridge nonlinear science series 7. Cambridge university press, pp. 72–75.

Kennel MB, Brown R, Abarbanel HDI (1992) Determining embedding dimension for phase-space reconstruction using a geometrical construction. Physical Review A 45: 3403–3411.

Lee HS, Billings HJ, Lehman MN (2003) The suprachiasmatic nucleus: A clock of multiple components. Journal of Biology Rhythms 18: 435–449.

Lewis J, Glass L (1992) Nonlinear dynamics and symbolic dynamics of neural networks. Neural Computation 4: 621–642.

Liu C, Weaver DR, Strogatz SH, Reppert SM (1997) Cellular construction of a circadian clock: Period determination in the suprachiasmatic nuclei. Cell 91: 855–860.

Lontin A (1993) Nonlinear forecasting of spike trains from sensory neurons. International Journal of Bifurcation and Chaos 3: 651–661.

Lovejoy LP, Shepard PD, Canavier CC (2001) Apamin-induced irregular firing in vitro and irregular single-spike firing observed in vivo in dopamine neurons is chaotic. Neuroscience 104: 829–840.

Mckenna TM, Mcmullen TA, Shlesinger MF (1994) The brain as a dynamic physical system. Neuroscience 60: 587–605.

Meijer JH, Rietveld WJ (1989) Neurophysiology of the suprachiasmatic circadian pacemaker in rodents. Physiological Reviews 69: 671–707.

Moga MM, Moore RY (1997) Organization of neural inputs to the suprachiasmatic nucleus in the rat. Journal of Comparative Neurology 389: 508–534.

Moore RY, Silver R (1998) Suprachiasmatic nucleus organization. Chronobiology International 15: 475–487.

Moore RY (1996) Entrainment pathways and the functional organization of the circadian system. Progress in Brain Research 111: 103–119.

Moore RY, Speh JC (1993) GABA is the principal neurotransmitter of the circadian system. Neuroscience Letter 150: 112–116.

Morin LP (1994) The circadian visual system. Brain Research Reviews 19: 102–127.

Mpitsos GJ, Burton RM Jr, Creech HC, Soinila SO (1998) Evidence for chaos in spike trains of neurons that generate rhythmic motor patterns. Brain Research Bulletin 21: 529–538.

Newman GC, Hospod FE, Patlak CS, Moore RY (1992) Analysis of in vitro glucose utilization in a circadian pacemaker model. Journal of Neuroscience 12: 2015–2021.

Okamura H, Berod A, Julien JF, Geffard M, Kitahama K, Mallet J, Bobillier P (1989) Demonstration of GABAergic cell bodies in the suprachiasmatic nucleus: In situ hybridization of glutamic acid decarboxylase (GAD) mRNA and immunocytochemistry of GAD and GABA. Neuroscience Letter 102: 131–136.

Pennartz CM, De Jeu MT, Geurtsen AM, Sluiter AA, Hermes ML (1998) Electrophysiological and morphological heterogeneity of neurons in slices of rat suprachiasmatic nucleus. Journal of Physiology 506: 775–793.

Rabinovich MI, Abarbanel HID (1998) The role of chaos in neural systems. Neuroscience 87: 5–14.

Rapp PE, Albano AM, Schmah TI, Farwell LA (1993) Filtered noise can mimic low-dimensional chaotic attractors. Physical Review E 47: 2289–2297.

Rapp PE, Zimmerman ID, Vining EP, Cohen N, Albano AM, Jimenez-Montano MA (1994) The algorithmic complexity of neural spike trains increases during focal seizures. Journal of Neuroscience 14: 4731–4739.

Rapp PE, Zimmermann I, Albano A, Deguzman G (1985) Dynamics of spontaneous neural activity in the simian motor cortex. Physics Letter A 110: 335–338.

Reppert SM, Weaver DR (2002) Coordination of circadian timing in mammals. Nature 418: 935–941.

Reppert SM, Weaver DR (2001) Molecular analysis of mammalian circadian rhythms. Annual Reviews of Physiololgy 63: 647–676.

Rusak B (1977) The role of the suprachiasmatic nuclei in the generation of circadian rhythms in the golden hamster. Journal of Comparative Physiology 118: 145–164.

Sauer T (1994) Reconstruction of dynamical systems from interspike intervals. Physical Review Letters 72: 3811–3814.

Schaap J, Bos NP, de Jeu MT, Geurtsen AM, Meijer JH, Pennartz CM (1999) Neurons of the rat suprachiasmatic nucleus show a circadian rhythm in membrane properties that is lost during prolonged whole-cell recording. Brain Research 815: 154–166.

Schaap J, Pennartz CM, Meijer JH (2003) Electrophysiology of the circadian pacemaker in mammals. Chronobiology International 20: 171–188.

Schiff SJ, Jerger K, Chang T, Sauer T, Aitken PG (1994) Stochastic versus deterministic variability in simple neuronal circuits: II. Hippocampal slice. Biophysical Journal 67: 684–691.

Schreiber T, Schmitz A (2000) Surrogate data methods. Physica D 142: 346–382.

Schwartz WJ, Gross RA, Morton MT (1987) The suprachiasmatic nuclei contain a tetrodotoxin-resistant circadian pacemaker. Proceedings of National Academy of Sciences USA 84: 1694–1698.

Segundo JP (2003) Nonlinear Dynamics of Point Process Systems and Data. International Journal of Bifurcation and Chaos 13: 2035–2116.

Shadlen MN, Newsome WT (1998) The variable discharge of cortical neurons: Implications for connectivity, computation, and information coding. Journal of Neuroscience 18: 3870–3896.

Shen Y, Olbrich E, Achermann P, Meier PF (2003) Dimensional complexity and spectral properties of the human sleep EEG. Clinical Neurophysiology 114: 199–209.

Shibata S, Oomura Y, Hattori K, Kita H (1984) Responses of suprachiasmatic nucleus neurons to optic nerve stimulation in rat hypothalamic slice preparation. Brain Research 302: 83–89.

Shirakawa T, Honma S, Honma K (2001) Multiple oscillators in the suprachiasmatic nucleus. Chronobiology International 18: 371–387.

Softky WR, Koch C (1993) The highly irregular firing of cortical cells is inconsistent with temporal integration of random EPSPs. Journal of Neuroscience 13: 334–350.

Suzuki H, Aihara K, Murakami J, Shimozawa T (2000) Analysis of neural spike trains with interspike interval reconstruction. Biological Cybernetics 82: 305–311.

Takens F (1981) Detecting strange attractors in turbulence in dynamical systems and turbulence. Lecture Notes in Mathematics, 898: 366–381.

Theiler J (1986) Spurious dimensions from correlation algorithms applied to limited time-series data. Physical Review A 34: 2427–2432.

Theiler J, Eubank S, Longtin A, Galdrikian B, Farmer JD (1992) Testing for nonlinearity in time series: The method of surrogate data. Physica D 58: 77–94.

Troyer TW, Miller KD (1997) Physiological gain leads to high ISI variability in a simple model of a cortical regular spiking cell. Neural Computation 9: 971–983.

van Esseveldt KE, Lehman MN, Boer GJ (2000) The suprachiasmatic nucleus and the circadian time-keeping system revisited. Brain Research Reviews 33: 34–77.

Wan YH, Jian Z, Hu SJ, Xu H, Yang HJ, Duan YB (2000) Detection of determinism within time series of irregular burst firing from the injured sensory neuron. Neuroreport 11: 3295–3298.

Welsh DK, Logothetis DE, Meister M, Reppert SM (1995) Individual neurons dissociated from rat suprachiasmatic nucleus express independently phased circadian firing rhythms. Neuron 14: 697–706.